Control of III–V nanowire crystal structure by growth parameter tuning

2010 Semicond. Sci. Technol. 25 024009

(http://iopscience.iop.org/0268-1242/25/2/024009)

IOP PUBLISHING SEMICONDUCTOR SCIENCE AND TECHNOLOGY
Semicond. Sci. Technol. **25** (2010) 024009 (11pp) doi:10.1088/0268-1242/25/2/024009

Control of III–V nanowire crystal structure by growth parameter tuning

Kimberly A Dick[1,2,4], **Philippe Caroff**[1,3], **Jessica Bolinsson**[1],
Maria E Messing[1], **Jonas Johansson**[1], **Knut Deppert**[1],
L Reine Wallenberg[2] **and Lars Samuelson**[1]

[1] Departement of Solid State Physics, Lund University, Box 118, S-221 00 Lund, Sweden
[2] Departement of Polymer and Materials Chemistry/nCHREM, Lund University, Box 124, S-221 00 Lund, Sweden
[3] IEMN, UMR CNRS 8520, BP 60069, Avenue Poincaré, 59652 Villeneuve d'Ascq, France

E-mail: kimberly.dick@ftf.lth.se

Received 8 June 2009, in final form 28 July 2009
Published 22 January 2010
Online at stacks.iop.org/SST/25/024009

Abstract
In this work we investigate the variation of the crystal structure of gold-seeded III–V nanowires with growth parameters, in order to gain a cohesive understanding of these effects. We investigate six III–V materials: GaAs, InAs, GaP, InP, GaSb and InSb, over a variation of growth conditions. All six of these materials exhibit a cubic zinc blende structure in bulk, but twin planes and stacking faults, as well as a hexagonal wurtzite structure, are commonly observed in nanowires. Parameters which may affect the crystal structure include growth temperature and pressure, precursor molar fraction and V/III ratio, nanowire diameter and surface density, and impurity atoms. We will focus on temperature, precursor molar fraction and V/III ratio. Our observations are compared to previous reports in the literature of the III–V nanowire crystal structure, and interpreted in terms of existing models. We propose that changes in the crystal structure with growth parameters are directly related to changes in the stable side facets.

(Some figures in this article are in colour only in the electronic version)

1. Introduction

III–V materials exhibit many interesting electrical and optical properties that make them very good candidates for nanowire applications in several fields. Their high mobility can be used in vertical field effect transistors, where the electrostatic coupling with the wrap gates is optimal [1, 2]. Promising thermoelectric power generation has also been proposed for low bandgap III–V nanowires [3]. Nanowire-based lasers and single photon sources could also be of great potential [4]. Applications such as these require the highest level of control of the material crystal quality. However, III–V nanowires often show high densities of twin planes, stacking faults or uncontrolled polytypism (random changes of the crystal phase in a single nanowire).

In bulk, all III–V materials, with the exception of nitrides (III-N), exhibit a cubic zinc blende (ZB) structure. III-N materials instead exhibit the related hexagonal wurtzite (WZ) structure. However, nearly all III–V nanowires contain high densities of stacking faults and twin planes [5–7], and high-purity ZB nanowires are the exception rather than the rule [8–11]. Dominant WZ nanowires have been reported for GaAs [12–15] and InP [16, 17], and substantial WZ segments have been reported in GaP [18]. For InAs, the WZ structure seems to be far more common than the ZB structure, and virtually all nanowires are reported to crystallize in this phase [19–21]. Also, the ZB phase has been reported in GaN nanowires [22], which exhibit only the WZ phase in bulk.

This intermixing of the ZB and WZ structures is related to the direction in which most III–V nanowires grow. Growth most often occurs in the $\langle 1\,1\,1\rangle$ crystal directions in the cubic cell, which are very closely related to the $\langle 0\,0\,0\,1\rangle$ directions in the hexagonal cell. Both crystal structures are held together by tetrahedral bonds between the atoms and, as seen in figure 1, they very much resemble one another. In the $\langle 1\,1\,1\rangle$ crystal

---

[4] Author to whom any correspondence should be addressed.

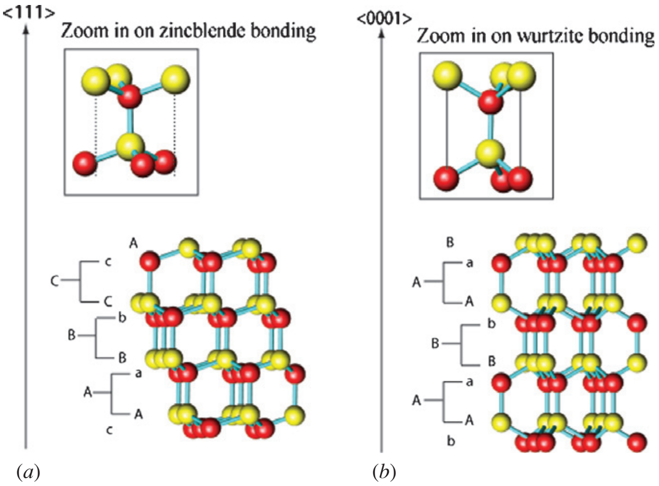

Figure 1. Stacking sequences in zinc blende (*a*) and wurtzite (*b*) crystal structures in the $\langle \bar{1}\,1\,0\rangle$ viewing direction. Different atom colours (shades) denote the two types of atoms (groups III and V), while upper and lowercase letters indicate layers of these two atoms types. The insets show zoomed-in views of the bonding configuration in the zinc blende and wurtzite structures. It is clear that the third-nearest-neighbour bond length is shorter in the wurtzite structure.

directions, the ZB crystal phase exhibits a repeated stacking sequence of three distinct layers of III–V pairs (figure 1(*a*)). The WZ crystal phase is on the other hand described by a stacking sequence of two distinct layers of III–V pairs (figure 1(*b*)). The energetic difference between these two crystal structures arises from the difference in the third-nearest-neighbour atom spacing, which is shorter for WZ than for ZB (insets, figures 1(*a*) and (*b*)). Since nanowires are believed to grow layer-by-layer in the growth direction, a small change in the sequence of the layers in the $\langle 1\,1\,1\rangle$ growth direction easily leads to a change between the WZ and ZB crystal structures.

Although the change in structure is subtle, it can have significant consequences for the properties of the resulting nanowires. It has been demonstrated that WZ and ZB phases in nanowires have different band structures [23–26]. A mixture of structures is therefore a challenge for optical applications [27–29]. For electronic applications, stacking faults and twin planes can act as scattering centres for electrons, again degrading performance [30, 31]. It is clear that a random mixture of phases and many stacking defects will limit the opportunities to develop future applications for III–V nanowires. On the other hand, the ability to selectively tune the crystal structure could be advantageous. The selective control of twin defects may even allow for interesting opportunities: Ikonic *et al* have shown theoretically that periodic twin-plane superlattices would yield effects such as mini-band formation and the opening of zero energy gaps at the superlattice Brillouin zone boundary [32, 33]. In addition to changes in the internal crystal structure, related changes in side facets may also be of interest. Moore *et al* have suggested that nanowires with periodically modulated side facets will exhibit low thermal conductivity due to phonon backscattering [34], making them very interesting for thermoelectric applications.

In this work we aim to provide a cohesive experimental investigation and understanding of the crystal structure of III–V nanowires. Following our earlier investigations of the structure of InAs [19], GaAs [35], GaP [18, 36], InSb [8, 37] and GaSb [38] nanowires, we have expanded the range of parameters investigated for these materials, and performed new investigations of InP nanowires. These results are discussed together with a thorough review of structure effects reported in the literature, and interpreted based on available theoretical models. We will focus on III–V nanowires seeded by Au particles, but much of the discussion could be applied to other particle types or particle-free growth techniques, as well as to other nanowire materials. Although the crystal structure is affected by a very wide range of growth parameters (discussed in section 3), we have chosen to focus our investigations on temperature, precursor molar fraction and V/III ratio, since extensive theoretical and experimental studies are available for comparison.

We propose that variations in the observed crystal structure can be interpreted in terms of changes in the side facets. The stable facets and surface reconstructions will depend on growth conditions and nanowire diameter. Since layer-by-layer nanowire growth is believed to proceed via nucleation at the edge of the wire (along the three-phase boundary with the seed particle), the energies of the side facets will affect the wire nucleation [39–41]. We aim to show that the observed structure of III–V nanowires can be explained by several basic processes, and the large variations observed using different growth systems and parameters are entirely consistent with these processes.

2. Methods

All nanowires used in this study were grown by metal-organic vapour phase epitaxy (MOVPE). Nanowires were grown by a particle-assisted growth mechanism using gold aerosol nanoparticles as growth seeds [42]. Particle diameters were selected as 10, 20, 30, 40, 50, 60, 70 and 80 nm, and were deposited on [1 1 1]B-oriented III–V substrates (the same material as the nanowires unless otherwise noted) for each set of conditions used in this study, with a typical selected surface density of 0.2 μm^{-2}.

Nanowires were grown in two low-pressure MOVPE systems from Epiquip and Aixtron, at a system pressure of 100 mbar unless otherwise specified. The use of two growth systems allows us to minimize machine-dependent effects and to check the reproducibility of the results. Hydrogen carrier gas was used with a flow rate of 6 L min^{-1} for the Epiquip system and 13 L min^{-1} for the Aixtron system. The precursors used were trimethylgallium (TMGa), trimethylindium (TMIn), trimethylantimony (TMSb), arsine (AsH_3) and phosphine (PH_3). For some materials (particularly GaAs and GaP), a high-temperature annealing step under group V flow was sometimes used prior to growth; this was not observed to affect the crystal structure and is thus not discussed further. Growth times were selected in the range of 1–45 min to give appropriate nanowire lengths, typically between 500 nm and 2 μm. Growth temperatures in the range of 350–550 °C

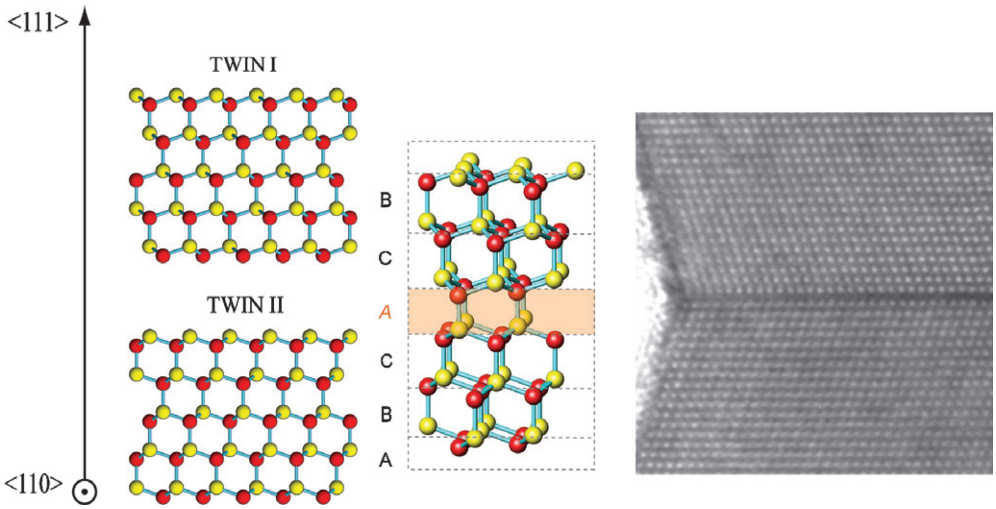

(*a*) (*b*) (*c*)

Figure 2. (*a*) Two different orientations of the zinc blende stacking sequence, denoted as 'I' and 'II'. (*b*) When the two orientations of zinc blende are combined, the common plane A is a twin plane or mirror plane. (*c*) Transmission electron microscopy image of a section of an InAs nanowire exhibiting two different orientations of zinc blende stacking (twin segments), separated by a twin plane. In the TEM image, group III and V atoms in adjacent plains cannot be resolved, and appear as a single dot.

were investigated, as specified in section 4. *In situ* cleaning using HCl gas and/or high temperature annealing followed by substantial dummy growth to cover reactor walls and liner was used in between material systems series.

Initial morphological characterization was performed using a field-emission scanning electron microscope (FEI Nova NanoLab 600), operated at 15 kV. Crystal structure characterization was performed using a JEOL-3000 F field-emission transmission electron microscope (TEM) operated at 300 kV. TEM images were recorded along the $\langle \bar{1}\,1\,0\rangle$ zone axis (cubic notation), using a 2k × 2k CCD camera. Samples for high resolution TEM were obtained by breaking off the nanowires from the substrate and transferring them to lacey carbon-film coated copper TEM grids. The determination of the nanowire side facet orientation was performed by combining TEM analysis with independent SEM observations of the hexagonal facet orientation of the as-grown nanowires with respect to the $\{1\,1\,0\}$ cleavage planes of the (1 1 1) B substrates.

3. Background

3.1. Description of structure

Before describing the growth results, it is necessary to fully describe the structures to be investigated. As mentioned above, ZB (or sphalerite) and WZ differ only in their stacking sequence in the close-packed directions ($\langle 1\,1\,1\rangle$ in the cubic structure and $\langle 0\,0\,0\,1\rangle$ in the hexagonal structure) [43]. This stacking sequence can be denoted as …CABCA… for ZB, where each letter represents one of the three possible positions of the pairs of group III and group V atomic layers aligned in the specific $\langle 1\,1\,1\rangle$ direction. For the WZ structure, only two possible positions are occupied, giving the notation …BABAB…. Alternatively, each atomic layer can be denoted separately using lower case and upper case letters for the two different atom species. The ZB and WZ stacking sequences are then written as …cAaBbCcA… and ……bAaBbAaB…, respectively (see figure 1). In situations where the structures are intermixed and/or different faults in their stacking sequence arise, this more detailed notation can be necessary to fully describe and distinguish between different defects and faults in the stacking sequence of these two types of crystal structures [44]. In this work we will refer to segments as 'extended' if either the ZB or WZ stacking sequence continues uninterrupted for at least 10 nm.

Often the ZB stacking sequence is found to suddenly change from an …ABCABC… stacking sequence to an …ABC$\underline{A}$CBACBA…. The stacking sequence is still ZB-type stacking after '$\underline{A}$', but the sequences before and after this bilayer are mirrored in '$\underline{A}$'. The 'mirror' plane '$\underline{A}$' is called a twin plane and the segments above and below '$\underline{A}$' have different twin orientations (figure 2). However, the small part of the sequence surrounding the twin plane could also be viewed as following a WZ-type stacking sequence. In this paper we exclusively use the terms twin and twin plane for this type of defects or interruption in the stacking sequence. We use the term WZ only when the WZ-type stacking sequence occurs over at least four bilayers. We use the term stacking faults to refer to interruptions in the WZ stacking sequence: …ABAB$\underline{C}$BABA… where $\underline{C}$ is the misplaced bilayer creating the stacking fault.

The energetic difference between ZB and WZ structures arises from the third-nearest-neighbour spacing, which is shorter in WZ. III–V materials have ionic bonds between the group III and V atoms, favouring a short bond length; however, steric hindrance tends to favour longer bond lengths. Although calculations of ionicity vary [45, 46], it is generally accepted that nitrides have the highest ionicity while antimonides have the lowest [47]. WZ is thus the favoured structure in small, ionic nitride materials, while ZB is favoured in other III–Vs. Yamashita *et al* considered the effect of ionicity on the prevalence of WZ in ZB nanowires [47]. They demonstrate that the least ionic materials (antimonides) exhibit the lowest density of twin defects, while more ionic materials have more twin defects.

Several theoretical models have addressed the occurrence of the WZ phase and ZB–WZ polytypism in nanowires of semiconductors that exhibit only the ZB structure in bulk. What these models have in common is an assertion that the high surface-to-volume ratio of nanowires is responsible for stabilizing the WZ structure. Specifically, all propose that the surface energies of nanowire side facets can be (or must be) low when the nanowire structure is WZ. If nanowires are small enough, then this surface energy can dominate, such that the equilibrium structure is changed. Also, if nucleation occurs at the edge of the particle–wire interface (triple line or three phase boundary; this assertion is justified in [39, 40]), then the surface or edge energy will affect the nucleation barrier.

3.2. Thermodynamics of a nanowire structure

Akiyama *et al* considered the thermodynamic stability of III–V nanowires of WZ and ZB structures [48]. They compare surface energies of WZ $\{\bar{1}100\}$ and ZB $\{\bar{1}10\}$ facets, and demonstrated that the WZ facets have a lower energy. Since the surface energy will dominate as diameter decreases, this led them to predict critical diameters below which WZ will be the stable structure. Galicka *et al* extended this idea to consider reasonable surface reconstructions as well as different growth directions [49]. In both cases the predicted critical diameters are too small to account for the observations of the WZ phase in III–V nanowires, but this approach is useful as a qualitative explanation for the stability of WZ.

Several groups have considered the relative stability of ZB and WZ nanowires with different side facets. Cahangirov and Ciraci performed first-principles calculations of the cohesive energy of thin GaAs nanowires: ZB nanowires with $\{\bar{1}10\}$ or $\{11\bar{2}\}$ facets and WZ nanowires with $\{\bar{1}100\}$ or $\{11\bar{2}0\}$ facets [25]. They determine that the cohesive energies for very small relaxed nanowires are highest for WZ, particularly with $\{\bar{1}100\}$ facets. They predict critical diameters of approximately 30 nm. On the other hand, Leitsmann and Bechstedt calculate that ZB nanowires with $\{\bar{1}10\}$ facets and WZ nanowires with $\{11\bar{2}0\}$ facets will be most stable [50]. However, they also indicate that in an atmosphere containing high concentrations of passivating species, WZ nanowires with $\{\bar{1}100\}$ facets will be most stable, followed by ZB nanowires with $\{11\bar{2}\}$ facets. The applicability of such results is not clear, however, especially since they consider only very small nanowire diameters. The most interesting result is that growth conditions can influence the stable side facets and stable crystal structure.

Dubrovskii *et al* have revisited the question of thermodynamic stability of nanowires by explicitly considering a variety of related polytypes, in addition to WZ and ZB [51]. They show that the 4H polytype (ABCB) should be regarded as the most stable structure for III–V nanowires. Moreover, they demonstrate that nanowires are inherently metastable (since the high surface area makes their formation energetically unfavourable), so growth is controlled by kinetics rather than thermodynamics. The authors indicate that their thermodynamic analysis is useful primarily for understanding the energetics of the nanowire structure.

3.3. Nucleation kinetics in nanowires

Several groups have considered the nucleation kinetics in III–V nanowires. Johansson *et al* proposed that twin plane formation can be explained using classical nucleation theory [36]. They demonstrated that the energy difference between a ‘normal’ and ‘twin’ nucleus should be small, and that the distribution of twin planes should therefore follow a geometrical distribution. The energy barrier to twin formation will be overcome more often by thermal fluctuations as temperature increases, so an increase in twin-plane density with temperature is expected. Extended WZ segments are not described by this model, although it is noted that when twin plane density is high there is a reasonable probability of two or more twin planes occurring in sequence.

Glas *et al* also use classical nucleation theory, in this case to describe the formation of the WZ phase in III–V nanowires [39]. They demonstrate that twin nucleation can be favourable if and only if nucleation occurs at the nanowire edge (triple line or three-phase boundary). If twin nucleation is favoured, extended WZ will be the result. A distribution of the WZ and ZB phases is still expected, since the energy difference between the two nuclei will still be small. An important point to note from both of the above papers is that any small fluctuations in the system can give rise to twin-plane nucleation; these might be thermal fluctuations, fluctuations in supply due to mass transport or fluctuations in the seed particle, perhaps in composition [52] or wetting angle.

Johansson *et al* model the relationship between supersaturation and twin nucleation probability, demonstrating that an increase in supersaturation should give an increase in twin planes [18]. They demonstrate experimentally that a significant decrease in supersaturation (of Ga for GaP nanowire growth) can dramatically reduce the density of twin planes. They note that the average WZ segment length is closely related to the probability of twin plane formation if at least two sequential twin planes are required to form the WZ phase, and discuss the necessary relative surface (edge) energies required to form extended WZ segments of a given length.

A recent work by Dubrovskii *et al* aims to provide a cohesive model of the nanowire crystal structure incorporating various effects [53]. This includes both a diameter dependence of crystal structure (arising from the Gibbs-Thomson effect) and the occurrence of the WZ phase as supersaturation is increased. They indicate that low proportions of the WZ phase should be favourable at low supersaturation, while high proportions (approaching 1) will be favourable at high supersaturation. The authors indicate that this trend is consistent with GaAs nanowires grown by molecular beam epitaxy (MBE) (see also [39]). One stated aim of this work was to predict the proportions in which the ZB and WZ phases should be stable, as a function of growth conditions.

The model predicts appropriate supersaturation levels for various structural results. Unfortunately, however, it is not straightforward to determine or control the supersaturation during nanowire growth.

3.4. Supersaturation during nanowire growth

Supersaturation is defined as the difference in chemical potential between the supply phase and the growing phase. For nanowires, growth occurs at the interface between the particle and wire, so we are interested in the chemical potential difference between supply atoms and this surface. This will be affected by temperature, pressure and the concentration of the supply atoms at the interface. Supersaturation of growth species is most directly controlled by varying the precursor molar fractions, and in most cases variation in total molar fraction can be interpreted cautiously as a variation in supersaturation. But it is important to understand that supersaturation is affected by many other growth parameters. As noted above, it depends on temperature and pressure; generally the chemical potential difference between a vapour and a solid phase will decrease with temperature. However, for growth techniques that involve molecular precursors, the decomposition of precursors typically increases exponentially with temperature, which increases the supersaturation for fixed precursor molar fractions. Additionally, surface reconstructions may vary with temperature and vapour molar fractions, in turn affecting the diffusion of adatoms.

Nanowire systems are even more complicated. For example, when growth is diffusion limited, adjacent nanowires compete for material and the supersaturation per nanowire is reduced [53]. Enhanced wire growth rate can also lead to locally decreased supersaturation [11]. Supersaturation will generally decrease as the nanowire grows and the surface collection area shrinks; it has been reported that the InP nanowire crystal structure changes as nanowires grow away from the substrate [54]. Also, the supersaturation decreases with increasing diameter within the diffusion-limited regime [53]. Local variation in precursor decomposition will also affect supersaturation; in this way it has been proposed that supersaturation will increase with nanowire surface density if seed particles act as catalysts [55]. Other factors may include the solubility of the seed particle (which can change with temperature) and trace impurities in the system (which may affect adsorption, diffusion and dissolution kinetics) [18, 56]. It has in fact been reported that dramatic changes in the crystal structure of InP nanowires occur when they are doped [56, 57].

For binary materials, such as III–V semiconductors, two different species (the group III and V elements) must combine to form the semiconductor material. These two species are controlled independently and follow different kinetic processes. They have different adsorption, diffusion and desorption rates on the semiconductor surface, which will affect their individual supersaturations at the growth interface. When molecular precursor species are used, the two different precursor molecules will have different decomposition kinetics, and may compete for reactants, or react with each other. It is not straightforward to determine the optimum ratio of precursor molar fractions required to obtain equal adatom concentrations of the two species at the growth interface. Therefore, the *molar fraction ratio* between the two species (V/III ratio) is an important parameter. At present, however, there is no model explaining the anticipated effect of the V/III ratio on the crystal structure.

It is clear that precursor molar fractions and the V/III ratio are related, but distinct, parameters affecting growth. For example, Joyce *et al* showed that the density of twin planes in GaAs ZB nanowires decreases when the two precursors are increased simultaneously (constant V/III ratio) [58] and when the As precursor is increased while the Ga is fixed (increased V/III ratio) [59]. However, it can be observed from their data that the density of twin planes most often seems to decrease if the Ga precursor is decreased for constant As (again, the increased V/III ratio). Given the possible large error bars in the data due to the twin density being very low, this seems to suggest that the V/III ratio has effects on the structure independent of total precursor concentration.

3.5. Further effects

In addition to temperature and chemical potential, phase stability and equilibrium will be determined by the absolute pressure of the growth system. This is an important factor since growth pressures vary widely (from UHV almost to atmospheric pressure). We have observed that the morphology of InP nanowires changes drastically with a fivefold increase in pressure [19]. However, to our knowledge there are no experimental or theoretical studies of the effect of pressure on the nanowire crystal structure. Thus, apart from noting its possible effect, we will not discuss it in this paper.

All the models discussed above describe the variation in the structure for fixed values of WZ and ZB surface/edge energies. The aim has been to show that the WZ structure or polytypes may be stabilized by low surface/edge energies. However, it is also important that the surface energies vary in different ways with temperature, pressure and molar fraction, even for the same material and structure. We should even expect the occurrence of different surface reconstructions, as is the case for planar surfaces. Therefore, the lowest-energy surface may change at certain critical values of these parameters, abruptly changing the resulting structure and morphology. Investigations of the surface structure of nanowires as a function of environment will be of great interest. To date only very few (post-growth) studies have been attempted [60, 61], and these most likely do not represent the *in situ* surface reconstructions.

One final point that should be considered is the seed particle used for nanowire growth. The models above are intended to be general, and do not explicitly consider the particle material. Most could in principle also be applied to particle-free growth. However, Soshikov *et al* [62] note an epitaxial relationship between the particle phase and WZ GaAs nanowires, and suggest that the particle phase influences the wire structure. It has similarly been observed that antimonide nanowires have epitaxially matched $AuIn_2$ and $AuGa_2$ particles [8, 38]. Changes in the particle structure with conditions (for example, from solid to liquid with increasing temperature) may affect the nanowire crystal structure. It has also been proposed that incorporation of impurity atoms into the particle will affect dissolution kinetics and therefore supersaturation [18]. Also, Akiyama *et al* [63] propose that the WZ structure can be stabilized in GaAs nanowires grown with Au particles, by incorporation of Au atoms into the structure. It is not yet clear what predictions can be made using these effects, but the possibilities should be kept in mind.

We now turn to the experiments, designed to extend and complete earlier investigations of the preferred crystalline phase in standard III–V nanowire material systems.

4. Results

4.1. InSb and GaSb

InSb and GaSb nanowires have been grown as heterostructure segments on GaAs, InAs and InP nanowire templates [37]. TEM investigations indicated that these nanowires exhibited a pure ZB crystal structure free of stacking faults or twin defects. It was also observed that the nanowires have a hexagonal cross-section with $\{\bar{1}\,1\,0\}$ side facets. More extensive TEM characterization has shown that the reported structure and morphology are not affected by growth parameters over the entire investigated parameter space accessible in our systems. InSb nanowires have been grown at temperatures from 400 to 480 °C, and molar fractions from 2.7×10^{-6} to 1.0×10^{-5} and from 5.0×10^{-6} to 2.5×10^{-4}, respectively, for TMIn and TMSb. GaSb nanowires have been grown at molar fractions from 5.0×10^{-6} to 4.0×10^{-5} and from 1.6×10^{-5} to 6.1×10^{-5}, respectively, for TMGa and TMSb. Also, no influence of substrate material on the crystal structure has been observed.

4.2. GaAs

The crystal structure of GaAs nanowires has been investigated over the temperature range of 350–550 °C (figure 3). Using molar fractions of 1.3×10^{-5} (TMG) and 5.5×10^{-4} (AsH_3), we have observed that nanowires grown at low temperature exhibit a ZB crystal structure with low-density twin planes (figure 3(*a*)). As temperature is increased, twin plane density increases, with stacking faults (short WZ segments) first appearing around 450 °C (figures 3(*b*), (*c*)). At sufficiently high temperature (around 550 °C), the WZ structure begins to dominate the nanowire (figure 3(*d*)). A transition from the mixed structure to pure WZ is observed by Plante *et al* [14] over the temperature range of 500–600 °C in MBE, showing that the same trend holds even though other growth conditions are very different. Another important observation is that GaAs nanowires with the predominantly WZ structure generally exhibit the ZB structure in the region directly under the particle ('neck region') [13, 39]. This is usually attributed to a decrease in Ga supersaturation after the Ga precursor is turned off.

The side facets of GaAs nanowires with the highly twinned ZB structure consist of $\{1\,1\,1\}$-oriented microfacets [35], such that nanowire segments take the form of octahedral slices. The same structure has been reported for GaAs nanowires grown by MBE [64]. However, it is clear from the model that segment length cannot extend infinitely with such inclined side facets, since the nanowire cross-section decreases as the nanowire grows [36, 56]. We have observed that extended ZB segments in GaAs nanowires exhibit $\{1\,1\,\bar{2}\}$-oriented facets (figure 3(*a*)). Close inspection reveals that facets are initially oriented in $\{1\,1\,1\}$ directions following a twin plane, but switch to the $\{1\,1\,\bar{2}\}$ orientation after a certain segment thickness, without the formation of any obvious defect. We also note that nanowires grown in the $\langle 1\,1\,1\rangle$A directions, which are free of twins and stacking faults, have $\{1\,1\,\bar{2}\}$ facets [11]. An interesting effect is that extended ZB twin segments alternate with very short (~5 nm) twin segments; in other words there appears to be a favoured twin segment orientation (also reported in [65]). This favoured orientation does not correspond to a specific direction, since adjacent nanowires may have different favoured orientations and a change in favoured orientation may occur within a single nanowire. Finally, we observed that WZ segments in GaAs nanowires have side facets oriented towards the $\{\bar{1}\,1\,0\,0\}$ direction in the hexagonal cell.

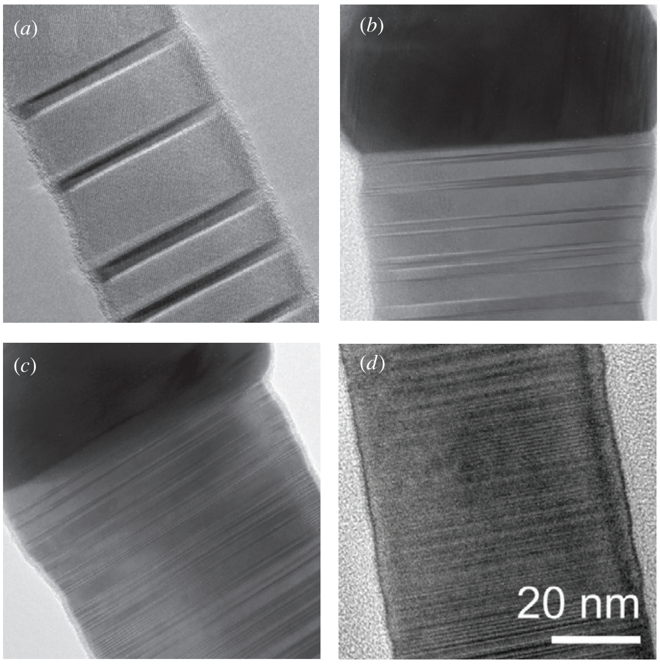

Figure 3. TEM images showing GaAs nanowires in the $\langle\bar{1}\,1\,0\rangle$ viewing direction, grown with molar fractions of 1.3×10^{-5} (TMG) and 5.5×10^{-4} (AsH_3) at (*a*) 350 °C, (*b*) 400 °C, (*c*) 500 °C and (*d*) 550 °C. The wires grow in the $[\bar{1}\,\bar{1}\,\bar{1}]$ direction; for consistency the growth direction is upwards in all figure panels. In (*a*) the wire exhibits a zinc blende structure, but with several twin planes separating segments of different orientation. It is clear that one segment orientation (brighter contrast) is favoured over the other (darker contrast). The twin plane density increases in (*b*) and (*c*), with (*c*) also exhibiting some thin wurtzite segments. The wire in (*d*) exhibits fairly equal proportions of zinc blende and wurtzite.

4.3. GaP

We have reported a very similar temperature effect for GaP [36], with twin plane and stacking fault density increasing with temperature. The effect of supersaturation has also been investigated for this material, by 'pulsing' the Ga precursor source such that the concentration of supply atoms at the interface fluctuated [18]. We observed that lowering the Ga supersaturation (for a constant P supersaturation) decreases the twin plane density substantially (a very similar result is reported in [66]). It was not clarified whether this effect is due to absolute or relative supersaturation (V/III ratio). However, the direction of change is the same as that demonstrated by Joyce *et al* [58, 59] if the Ga precursor is varied independently (decreasing V/III ratio) but not if both precursors are varied (constant V/III ratio). Also, the WZ structure was reported for nanowires grown in very clean conditions, attributed to a much higher Ga supersaturation. GaP nanowires exhibit the same side facet types as GaAs nanowires under the conditions investigated: $\{1\,1\,1\}$ microfacets for short ZB segments, $\{1\,1\,\bar{2}\}$ facets for longer ZB segments and $\{\bar{1}\,1\,0\,0\}$ facets for WZ segments. GaP nanowires with diameter above 100 nm also have a low density of twin planes compared to thinner nanowires grown under the same conditions. We will not discuss this here, except to note that once again, $\{1\,1\,\bar{2}\}$ facets are observed. Also, there appears to be a favoured twin segment orientation.

4.4. InAs

InAs has been investigated over the temperature range of 370–480 °C. This material also exhibits a significant effect of diameter on crystal structure, with very thin nanowires being entirely WZ [19, 21] and very large diameter nanowires entirely ZB [21]. This will not be discussed in detail here, except to note that the ability to tune structure with diameter allows access to a much larger structure range, greatly facilitating the investigation of other growth parameter effects.

For temperatures from 400 to 480 °C, InAs shows a shift from the predominantly WZ structure towards the predominantly ZB structure. Here the diameter effect is useful, since it allows us to tune the structure from pure WZ to pure ZB using only temperature. By varying the diameter we can see that the structure variation with temperature extends over the entire range (WZ to ZB) [21]. At lower temperatures, a very interesting effect is observed. From 370 to 390 °C, the nanowires exhibit a predominantly ZB structure, with twin plane and stacking fault densities increasing with temperature. This trend is exactly opposite to that observed for higher temperature. There is a sharp discontinuity in the temperature dependence between 390 and 400 °C, when the structure switches from very predominantly ZB to nearly pure WZ (figure 4). One very interesting effect is that the neck region of ZB nanowires contains first a short WZ segment, then a short ZB segment (figure 4(*a*)); this structure was observed for all nanowires investigated at 390 °C or below. On the other hand, the WZ nanowires grown at 400 °C have a short ZB neck region (figure 4(*c*)).

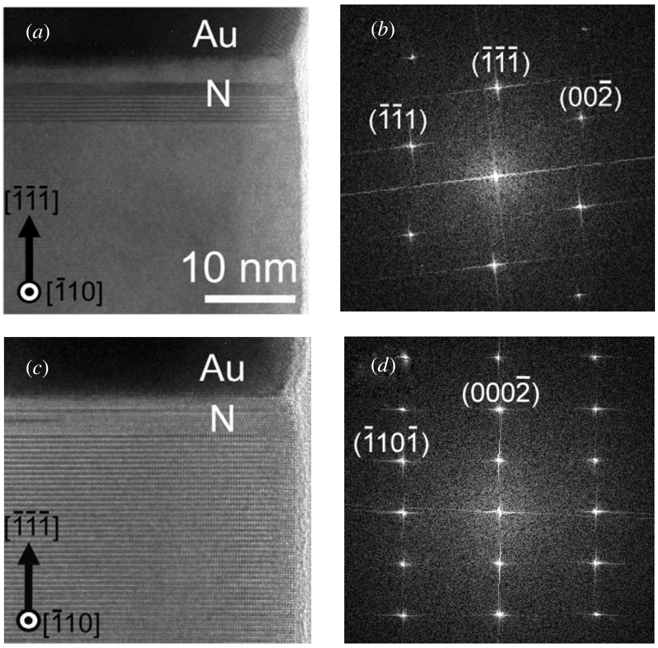

Figure 4. TEM images in the $\langle\bar{1}\,1\,0\rangle$ viewing direction of InAs nanowires grown at (*a*) 390 °C and (*c*) 400 °C. The wire in (*a*) has a zinc blende structure as seen in the FFT (*b*), while the wire in (*c*) has a wurtzite structure (*d*). It is also clear in both images that the region directly below the gold particle ('neck region', N) has the opposite crystal structure. The FFTs are taken over the entire wire below the indicated neck region.

InAs also exhibits interesting behaviour when the predominantly structure is ZB. At low temperatures (370–390 °C), the nanowires tend to have only low-density twin planes and $\{1\,1\,\bar{2}\}$-type side facets. However, when the ZB structure is exhibited at higher temperatures (for large diameters at temperatures above 400 °C), the nanowires adopt a periodically twinned morphology (figure 5(*a*)–(*d*)), with segments bounded by $\{1\,1\,1\}$-type facets [21]. However, when nanowires become sufficiently large at these higher temperatures (beyond the periodically twinned regime), they are twin free and exhibit $\{\bar{1}\,1\,0\}$ side facets. At the threshold to this regime, full octahedrons may be observed within an InAs nanowire with (otherwise) $\{\bar{1}\,1\,0\}$ facets (figure 5(*e*)). InAs nanowires with the WZ structure are always observed to exhibit $\{\bar{1}\,1\,0\,0\}$ facets.

4.5. InP

The effects of temperature, molar fraction and V/III ratio have been investigated for InP nanowires. We observe that the predominantly crystal structure changes from ZB at 380 °C to WZ at 430 °C, for molar fractions of 4.6×10^{-6} (TMIn) and 3.8×10^{-5} (AsH_3). However, interpretation of this effect must be made with care. We have also observed, for InP nanowires grown at 430 °C and V/III ratio of 207, that the total molar fraction affects the crystal structure. Nanowires grown at the highest molar fractions exhibit the mixed WZ and ZB structure, while nanowires grown at the lowest molar fractions exhibit the WZ structure with low-density stacking faults (figure 6). This effect was not observed for the lower temperature. Additionally, we observed that nanowires grown at 430 °C with a reduced V/III ratio were entirely ZB with dense twin planes (figure 6(*d*)). Paiman *et al* [17] have in fact observed that InP nanowires adopt a ZB structure at a low V/III ratio, changing towards WZ as the V/III ratio is increased. We

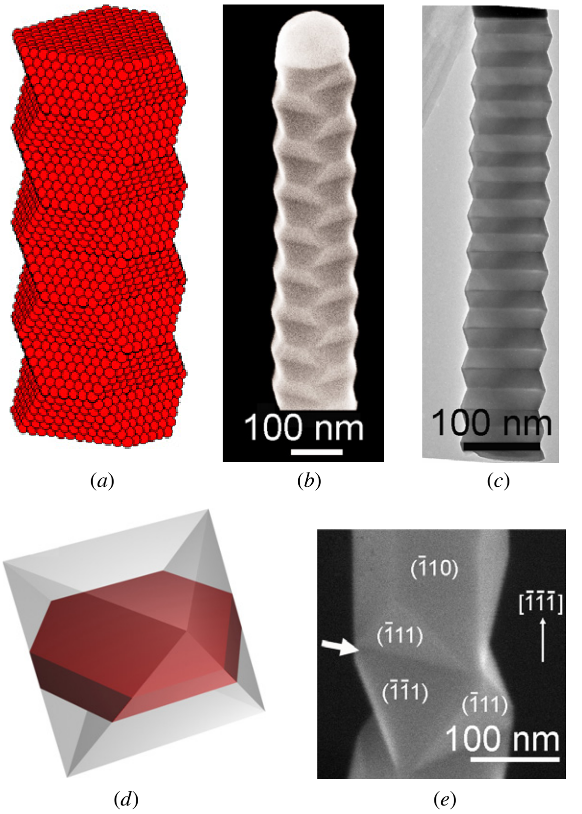

Figure 5. Nanowire facet structure (*a*) 3D model of a nanowire with $\{1\,1\,1\}$ microfacets. Examples of InAs nanowires exhibiting this facet structure are shown by SEM (*b*) and TEM (*c*). The model is composed of octahedral slices, of the type shown in (*d*). The thickness of the octahedral slices varies with growth conditions, up to the limit of a full octahedron. (*e*) SEM image of an InAs nanowire containing a full octahedron, with some of the $\{1\,1\,1\}$-type facets labelled. The thick arrow indicates the twin plane following an octahedron. Beyond the octahedron, the side facets of this nanowire convert to $\{1\,1\,0\}$ type.

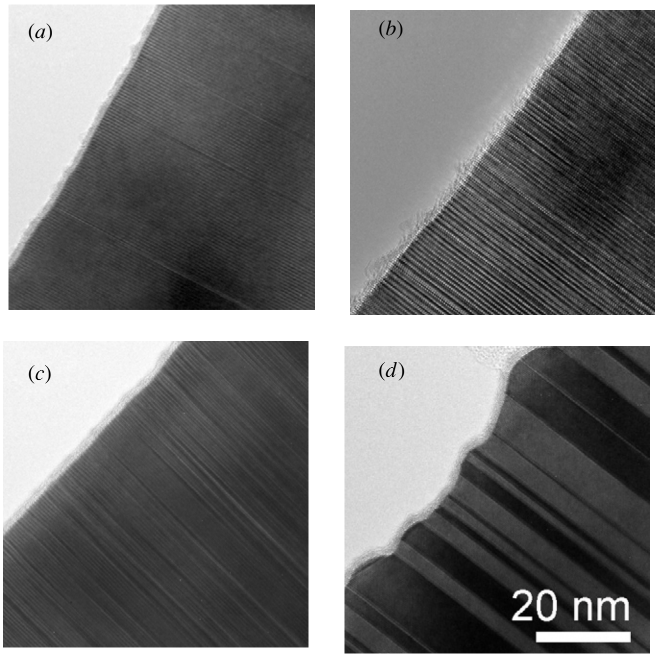

Figure 6. TEM images of InP nanowires in the $\langle \bar{1}\,1\,0\rangle$ viewing direction, grown with varied precursor molar fractions. The wires grow in the $[\bar{1}\,\bar{1}\,\bar{1}]$ direction; for consistency the growth direction is upwards in all figure panels. (*a*) Wire grown at 4.5×10^{-6} TMIn, 9.4×10^{-3} PH_3 (V/III = 207), which exhibits a wurtzite structure with occasional stacking faults. (*b*) Wire grown at 3.4×10^{-5} TMIn, 7.1×10^{-3} PH_3 (V/III = 207), exhibiting a higher stacking fault density than in (*a*). (*c*) Wire grown at 1.2×10^{-4} TMIn, 2.5×10^{-2} PH_3 (V/III = 207), which exhibits a predominant wurtzite structure but has high density of stacking faults. Note that the molar fractions have been increased by a factor of 30 to achieve this variation. (*d*) Wire grown at a reduced V/III of 83 (6.9×10^{-5} TMIn, 5.7×10^{-3} PH_3), which exhibits a twinned zinc blende structure.

noted that InP nanowires with the predominantly ZB structure (those grown at lower temperature or decreased V/III ratio) often exhibit a WZ neck region. InP is also reported to exhibit a diameter dependence, with increasing WZ structure as the diameter decreases [17].

Extended ZB InP segments were not observed under the conditions used here (although they are reported in the literature [17]). The side facets of short ZB segments (separated by high-density twin planes) were observed to be $\{1\,1\,1\}$ oriented. As for other materials, WZ segments had $\{\bar{1}\,1\,0\,0\}$ side facets.

5. Discussion

5.1. Trends in the crystal structure

Our observations indicate that the effects of growth parameters on the crystal structure are complicated and must be interpreted carefully. Growth temperature, for example, is a ‘simple’ parameter to vary and there are many reports of its effect on the structure. However, two completely opposite effects have been observed: first, nanowires grown at lower temperature may be predominantly ZB and exhibit an increased WZ phase at higher temperature, or second, nanowires may be WZ at lower temperature and increasingly ZB at higher temperature. Our observation of both of these effects for InAs (within different temperature ranges) clearly shows that this is not a material-specific effect. The abruptness of the switch between these two trends for InAs (over at most 10 °C) suggests that this effect is linked to thermodynamics, not to kinetics. This could be a change in the particle phase, or more probably in nanowire surface reconstruction, such that the side facet energies change significantly, and the lowest-energy surface changes.

Models of the crystal structure based on nucleation kinetics indicate that the mixed ZB and WZ structure in nanowires occurs because the energy difference between the two critical nuclei is small. Increased temperature or supersaturation results in larger energy fluctuations, and so both orientations occur with a statistical distribution. If the energy difference between the two types of nuclei becomes insignificant (at elevated temperature or supersaturation), a completely random mixture of the two structures will result. An increase in stacking faults within the predominantly phase (from pure ZB to completely mixed WZ and ZB, as is reported here for GaAs with increasing temperature) is explained by this effect. Within a reasonable supersaturation window, a transition from essentially pure ZB to essentially pure WZ is predicted with increasing supersaturation [53]. The appearance of the WZ phase can thus be interpreted as a 'high supersaturation' effect, where high molar fractions are generally taken to mean high supersaturation. The change of the structure to ZB in the neck region of WZ GaAs nanowires is consistent with this understanding, since the Ga supersaturation at the interface is expected to drop gradually after the precursor is turned off.

On the other hand, we have also observed the opposite effect for InP: nanowires transition from moderately pure WZ at low molar fraction to a mixture of WZ and ZB at very high molar fraction (increased by 30×). Also, WZ neck regions were often observed on ZB nanowires. These observations suggest that WZ is the stable/metastable phase under these conditions. It is important to note that the occurrence of WZ segments at the first place (in materials for which ZB is the stable bulk structure) is believed to relate to lower surface/edge energy for this structure. Since the total nucleation energy contains an 'interior' component (which favours ZB as the stable structure) and an 'edge' component (which may favour WZ if the surface/edge energy for this structure is lower), the relative magnitudes of these will determine which structure dominates under what conditions. If the edge energy for the WZ nucleus is sufficiently low compared to the ZB nucleus edge energy, it is possible that only WZ will be observed at the lowest achievable supersaturations, and the proportion of ZB will increase with supersaturation. Plante *et al* in fact observed that lowering the precursor molar fractions (simultaneously, such that the V/III ratio is maintained) resulted in very clean WZ GaAs nanowires [14].

Since values for the surface (edge) energies relevant to III–V nanowires are generally unknown, it is not possible, at present, to quantitatively predict the structure of these nanowires for given conditions. At best, qualitative discussion may be possible to explain the observed results. Also, changes in surface energies and reconstructions as a function of growth parameters cannot be discussed at present in a meaningful way. However, such effects should certainly occur, and a change in the lowest-energy surface for a particular set of conditions could result in an abrupt change of structure, most likely due to an abrupt change in surface reconstruction.

The abrupt change in the InAs crystal structure as the temperature is raised from 390 to 400 °C may be an example of this effect. Here, rather than a gradual increase in stacking faults, we see a complete change from nearly pure ZB to nearly pure WZ over a very small temperature interval. To explain this effect with existing models a change in input parameters is needed for these two temperatures. It is of course reasonable that surface energies change with temperature, and that the temperature variation of different surfaces will be different. Moreover, abrupt changes in surface reconstruction can occur. The opposite behaviour of the neck regions of InAs nanowires grown at these temperatures (as shown in figure 4) again suggests an abrupt change if the neck region represents a region of low supersaturation (as discussed above); this suggests that the stable structure is very sensitive to supersaturation under these conditions.

We must also consider one surprising observation for InAs: an increase in the ZB phase purity with temperature above 400 °C. We have already noted that, for low-to-moderate diameters, InAs nanowires exhibit the predominantly WZ phase, with increasing stacking faults as the temperature is increased. However, InAs also exhibits a strong diameter effect, and for large diameters the nanowires have a mixed WZ and ZB structure even at the lowest temperature (400 °C). For diameters above 100 nm, we observe that the WZ structure decreases with temperature, eventually giving periodically twinned ZB and, for the largest diameters, pure ZB nanowires. This is not easily explained with existing models.

The complete absence of stacking faults and twin defects in antimonides is of interest as well. As described above, Yamashita *et al* considered the prevalence of planar defects in ZB nanowires as a function of ionicity, showing that such defects should be least likely in antimonides [47]. However, their model does not predict perfectly clean antimonide materials, nor does it predict a dramatic difference in twin density compared to materials such as GaAs. This implies that ionicity alone may not be sufficient to explain the consistent crystal perfection observed. It must be emphasized here that reports of antimonide nanowire growth are extremely few compared with the other III–V materials discussed in this paper. Also, the accessible parameter ranges in this study are relatively small. Therefore, it may be that other structures would be possible in antimonide nanowires in other systems.

5.2. Relevance of observed facets

It is interesting that the most common facets for most III–V materials are of the $\{1\,1\,1\}$ type. These facets are low-index facets, but they are also polar and not parallel to the growth direction. None of the calculations of nanowire energetics for different side facet types consider $\{1\,1\,1\}$ microfacets. However, since microfacets necessarily increase the surface-to-volume ratio, it is reasonable that such a structure will not normally be lowest in energy. Leitsmann and Bechstedt indicate that under highly passivating conditions where ZB $\{1\,1\,\bar{2}\}$ and WZ $\{\bar{1}\,1\,0\,0\}$ facets are favoured, a high surface area should also be favoured [50]. It is not clear how realistic such conditions are, but the idea is intriguing.

It is also important to recall that since nanowires grow layer-by-layer, the side facets are built up as atoms stack in the growth direction. It is not necessarily obvious that the lowest-energy facets should form this way, as they would if the nanowires grew laterally. For comparison, we note that nanowire 'shells', which are grown laterally on pre-grown cores at elevated temperature, typically exhibit $\{\bar{1}\,1\,0\}$ facets regardless of the facets of the core [67, 68].

Since the $\{1\,1\,1\}$ facets are not parallel to the growth direction, maintenance of these facets as the wire grows results in a change in the cross-sectional area, specifically the particle–wire interface. It is obvious for purely geometrical reasons that this cannot continue forever; as the wire grows three of the six side facets will grow in area, while the other three will shrink (figure 5) [36, 56]. The degree to which this change in the interface area is tolerated will depend on the particle properties and phase, which may change abruptly with growth conditions. Eventually the wire may have a triangular cross-section, and if growth continued, the area would shrink to a point. However, since the particle must deform significantly as the interface area shrinks, it is not expected to be energetically favourable for the wire to shrink to a point. More realistically, when the strain reaches a certain critical level, a change in the facet structure must occur. One possibility is that a twin plane can form, switching the positions of the $\{1\,1\,1\}$ facets. Alternatively, a change in facet orientation can occur, to perhaps $\{1\,1\,\bar{2}\}$- or $\{\bar{1}\,1\,0\}$-type facets.

Interestingly, any of these situations may occur for different conditions. InAs, for example, exhibits extended ZB segments with $\{1\,1\,\bar{2}\}$ facets when grown at low temperature. However, at higher temperature (above 400 °C), ZB InAs has only $\{1\,1\,1\}$ microfacets and periodic twin planes. This indicates that the energy cost of forming $\{1\,1\,\bar{2}\}$ facets (which are not generally low-energy facets} is higher than the energy cost of forming a twin plane at these temperatures. For very large InAs nanowires grown at high temperatures, $\{\bar{1}\,1\,0\}$ facets are observed. This occurs when the octahedron is complete, as seen in figure 5.

The formation of $\{\bar{1}\,1\,0\}$ side facets is an interesting case, notable for its rarity. As stated above, it is expected that such facets should have the lowest energy, but they are not typically observed for axially grown nanowires. There are a few exceptions: InSb and GaSb nanowires always have $\{\bar{1}\,1\,0\}$ facets, as do very large InAs nanowires. Also, most Si nanowires are reported to have $\{\bar{1}\,1\;0\}$ facets. In all of these cases, nanowires have a perfect zinc blende (or diamond) structure free from stacking faults and twin planes. It seems reasonable to conclude that there is a relationship between the facets and the structural purity. It is not obvious, however, whether one causes the other or whether they have a common cause.

It is also clear that the particle–wire interface will not change when the WZ structure is formed, since all low-index facets will be parallel to the growth direction (due to the symmetry of the hexagonal cell). In cases where the nucleation energies of WZ and ZB are very close, this may help to stabilize the WZ structure. The energy cost of changing the area between the particle and wire should be included in the ZB nucleation energy. It is not at all obvious which side facets will be lowest in energy for nanowires of the WZ structure: the $\{\bar{1}\,1\,0\;0\}$ or $\{1\,1\;\bar{2}\,0\}$ facets. Both sets of facets are nonpolar and parallel to the growth direction, and first-principles calculations tend to give inconsistent results. However, in all of our investigations as well as in the literature, $\{\bar{1}\,1\,0\,0\}$ facets are observed. These facets are parallel to the cubic $\{1\,1\,\bar{2}\}$ facets, and it may therefore be natural to expect them on a wire which also has $\{1\,1\,1\}$ microfacets. The mechanism behind the selection of facets is not entirely clear however.

6. Conclusions

We have investigated the crystal structure of nanowires composed of six III–V materials-–GaAs, GaP, InAs, InP, GaSb and InSb-–and how it is determined by growth parameters including temperature and precursor molar fraction. These results are compared to the observations of the III–V nanowire crystal structure reported in the literature, and discussed in the context of current theoretical models. III–V nanowires frequently exhibit twin planes, stacking faults and polytypism, and these effects are believed to originate in the lower side facet energy of the hexagonal structure compared to the stable cubic structure. The structure is determined during growth by nucleation kinetics, and the similar nucleation energies for normal and twin nuclei give rise to the observed mixed crystal structures. Growth parameters will affect nucleation conditions, changing the overall structure. Also, we propose that since side facet energies and surface reconstructions are expected to change with growth parameters, the stable facets may change at critical parameter values, entirely changing the resulting crystal structure.

Acknowledgments

This work was carried out within the Nanometer Structure Consortium in Lund and was supported by the Swedish Foundation for Strategic Research (SSF), the Swedish Research Council (VR), the European Community (EU contract no 015783 NODE) and the Knut and Alice Wallenberg Foundation. This report is based on a project which was funded by E.ON AG as part of the E.ON International Research Initiative. Responsibility for the content of this publication lies with the authors.

References

[1] Thelander C, Fröberg L E, Rehnstedt C, Samuelson L and Wernersson L-E 2008 *IEEE Electron Device Lett.* **29** 206–8

[2] Cooke M 2006 Digital III-Vs review, III-Vs review vol 19, pp 18–22 (DOI: 10.1016/S0961-1290(06)71588-5)

[3] Zhou F, Seol J H, Moore A L, Shi L, Ye Q L and Scheffler R 2006 *J. Phys.: Condens. Matter* **18** 9651–7

[4] Zimmler M A, Bao J, Capasso F, Muller S and Ronning C 2008 *Appl. Phys. Lett.* **93** 051101

[5] Koguchi M, Kakibayashi H, Yazawa M, Hiruma K and Katsuyama T 1992 *Japan. J. Appl. Phys.* **31** 2061–5

[6] Johansson J, Wacaser B A, Dick K A and Seifert W 2006 *Nanotechnology* **17** S355–61

[7] Banerjee R, Bhattacharya A, Genc A and Arora B M 2006 *Phil. Mag. Lett.* **86** 807–16

[8] Caroff P, Wagner J B, Dick K A, Nilsson H A, Jeppsson M, Deppert K, Samuelson L, Wallenberg L R and Wernersson L-E 2008 *Small* **4** 878–82

[9] Joyce H J, Gao Q, Tan H H, Jagadish C, Kim Y, Zhang X, Guo Y and Zou J 2007 *Nano Lett.* **7** 921–6

[10] Krishnamachari U, Borgström M, Ohlsson B J, Panev N, Samuelson L, Seifert W, Larsson M W and Wallenberg L R 2004 *Appl. Phys. Lett.* **85** 2077

[11] Wacaser B A, Deppert K, Karlsson L S, Samuelson L and Seifert W 2006 *J. Cryst. Growth* **287** 504–8

[12] Dheeraj D L, Patriarche G, Zhou H, Hoang T B, Moses A F, Grønsberg S, van Helvoort A T J, Fimland B-O and Weman H 2008 *Nano Lett.* **8** 4459–63

[13] Persson A I, Larsson M W, Stenström S, Ohlsson B J, Samuelson L and Wallenberg L R 2004 *Nature Mater.* **3** 677–81

[14] Plante M C and LaPierre R R 2008 *Nanotechnology* **19** 495603

[15] Patriarche G, Glas F, Tchernycheva M, Sartel C, Largeau L and Harmand J-C 2008 *Nano Lett.* **8** 1638–43

[16] Moewe M, Chuang L C, Dubrovskii V G and Chang-Hasnain C 2008 *J. Appl. Phys.* **104** 044313

[17] Paiman S *et al* 2009 *Nanotechnology* **20** 225606

[18] Johansson J, Karlsson L S, Dick K A, Bolinsson J, Wacaser B A, Deppert K and Samuelson L 2009 *Cryst. Growth Des.* **9** 766–73

[19] Caroff P, Dick K A, Johansson J, Messing M E, Deppert K and Samuelson L 2009 *Nature Nanotech.* **4** 50–5

[20] Larsson M W, Wagner J B, Wallin M, Håkansson P, Fröberg L E, Samuelson L and Wallenberg L R 2007 *Nanotechnology* **18** 015504

[21] Shtrikman H, Popovitz-Biro R, Kretinin A, Houben L, Heiblum M, Bukała M, Galicka M, Buczko R and Kacman P 2009 *Nano Lett.* **9** 1506–10

[22] Jacobs B W, Ayres V M, Crimp M A and McElroy K 2008 *Nanotechnology* **19** 405706

[23] Trägårdh J, Persson A I, Wagner J B, Hessman D and Samuelson L 2007 *J. Appl. Phys.* **101** 123701

[24] Zanolli Z, Fuchs F, Furthmüller J, von Barth U and Bechstedt F 2007 *Phys. Rev.* B **75** 245121

[25] Cahangirov S and Ciraci S 2009 *Phys. Rev* B **79** 165118

[26] Maharjan A *et al* 2009 *Appl. Phys. Lett.* **94** 193115

[27] Bao J, Bell D C, Capasso F, Wagner J B, Mårtensson T, Trägårdh J and Samuelson L 2008 *Nano Lett.* **8** 836–41

[28] Pemasiri K *et al* 2009 *Nano Lett.* **9** 648–54

[29] Woo R L, Xiao R, Kobayashi Y, Gao L, Goel N, Hudait M K, Mallouk T E and Hicks R F 2008 *Nano Lett.* **8** 4664–9

[30] Stiles M D and Hamann D R 1990 *Phys. Rev* B **41** 5280–2

[31] Stiles M D and Hamann D R 1988 *Phys. Rev.* B **38** 2021–37

[32] Ikonić Z, Srivastava G P and Inkson J C 1994 *Surf. Sci.* **307–309** 880–4

[33] Ikonić Z, Srivastava G P and Inkson J C 1993 *Phys. Rev* B **48** 17181–93

[34] Moore A L, Saha S K, Prasher R S and Shi L 2008 *Appl. Phys. Lett.* **93** 083112

[35] Karlsson L S, Dick K A, Wagner J B, Malm J-O, Deppert K, Samuelson L and Wallenberg L R 2007 *Nanotechnology* **18** 485717

[36] Johansson J, Karlsson L S, Svensson C P T, Mårtensson T, Wacaser B A, Deppert K, Samuelson L and Seifert W 2006 *Nature Mater.* **5** 574–80

[37] Caroff P, Messing M E, Jeppsson M, Dick K A, Deppert K and Wernersson L-E 2009 *Nanotechnology* at press

[38] Jeppsson M, Dick K A, Wagner J B, Caroff P, Deppert K, Samuelson L and Wernersson L-E 2008 *J. Cryst. Growth* **310** 4115–21

[39] Glas F, Harmand J C and Patriarche G 2007 *Phys. Rev. Lett.* **99** 146101

[40] Wacaser B A, Dick K A, Johansson J, Borgström M T, Deppert K and Samuelson L 2009 *Adv. Mater.* **21** 153

[41] Nebol'sin V A and Shchetinin A A 2008 *Inorg. Mater.* **44** 1033–40

[42] Magnusson M H, Deppert K, Malm J-O, Bovin J-O and Samuelson L 1999 *Nano Struct. Mat.* **12** 45–8

[43] Bragg W L 1920 *Phil. Mag.* **39** 650

[44] Bolinsson J, Ouattara L, Hofer W A, Sköld N, Lundgren E, Gustafsson A and Mikkelsen A 2009 *J. Phys.: Condens. Matter* **21** 055404

[45] Abu-Farsakh H and Qteish A 2007 *Phys. Rev* B **75** 085201

[46] Christensen N E, Satpathy S and Pawlowska Z 1987 *Phys. Rev* B **36** 1032–50

[47] Yamashita T, Sano K, Akiyama T, Nakamura K and Ito T 2008 *Appl. Surf. Sci.* **254** 7668–71

[48] Akiyama T, Sano K, Nakamura K and Ito T 2006 *Japan. J. Appl. Phys.* **45** L275–8

[49] Galicka M, Bukała M, Buczko R and Kacman P 2008 *J. Phys.: Condens. Matter* **20** 454226

[50] Leitsmann R and Bechstedt R 2007 *J. Appl. Phys.* **102** 063528

[51] Dubrovskii V G and Sibirev N V 2008 *Phys. Rev* B **77** 035414

[52] Xiong Q, Wang J and Eklund P C 2006 *Nano Lett.* **6** 2736–42

[53] Dubrovskii V G, Sibirev N V, Harmand J C and Glas F 2008 *Phys. Rev* B **78** 235301

[54] Cornet D M, Mazzetti V G M and LaPierre R R 2007 *Appl. Phys. Lett.* **90** 013116

[55] Borgström M T, Immink G, Ketelaars B, Algra R and Bakkers E P A M 2007 *Nature Nanotech.* **2** 541–4

[56] Algra R E, Verheijen M A, Borgström M T, Feiner L–F, Immink G, van Enckevort W J P, Vlieg E and Bakkers E P A M 2008 *Nature* **456** 369–72

[57] Borgström M T, Norberg E, Wickert P, Nilsson H A, Trägårdh J, Dick K A, Statkute G, Ramvall P, Deppert K and Samuelson L 2008 *Nanotechnology* **19** 445602

[58] Joyce H J *et al* 2009 *Nano Lett.* **9** 695–701

[59] Joyce H J *et al* 2008 *Adv. Funct. Mater.* **18** 3794–800

[60] Hilner E, Håkanson U, Fröberg L E, Karlsson M, Kratzer P, Lundgren E, Samuelson L and Mikkelsen A 2008 *Nano Lett.* **8** 3978–82

[61] Ma D D D, Lee C S, Au F C K, Tong S Y and Lee S T 2003 *Science* **299** 1874

[62] Soshnikov I P, Cirlin G E, Tonkikh A A, Samsonenko Y B, Dubrovskii V G, Ustinov V M, Gorbenko O M, Litvinov D and Gerthsen D 2005 *Phys. Solid State* **47** 2213–8

[63] Akiyama T, Haneda Y, Nakamura K and Ito T 2009 *Phys. Rev* **B. 79** 153406

[64] Mariager S O, Sørensen C B, Aagesen M, Nygård J, Feidenhans'l R and Willmott P R 2007 *Appl. Phys. Lett.* **91** 083106

[65] Zou J, Paladugu M, Wang H, Auchterlonie G J, Guo Y N, Kim Y, Gao Q, Joyce H J, Tan H H and Jagadish C 2007 *Small* **3** 389–93

[66] Mohseni P K and LaPierre R R 2009 *Nanotechnology* **20** 025610

[67] Sköld N, Wagner J B, Karlsson G, Hernan T, Seifert W, Pistol M-E and Samuelson L 2006 *Nano Lett.* **6** 2743–7

[68] Keplinger M, Mårtensson T, Stangl J, Wintersberger E, Mandl B, Kriegner D, Holy V, Bauer G, Deppert K and Samuelson L 2009 *Nano Lett.* **9** 1877–82